

Observation of Quasi-Two-Dimensional Nonlinear Interactions in a Drift-Wave Streamer

T. Yamada,^{1,*} S.-I. Itoh,² S. Inagaki,² Y. Nagashima,¹ N. Kasuya,³ K. Kamataki,² H. Arakawa,⁴ T. Kobayashi,⁴ M. Yagi,² A. Fujisawa,² and K. Itoh³

¹*Graduate School of Frontier Sciences, The University of Tokyo, Kashiwa, Chiba 277-8561, Japan*

²*Research Institute for Applied Mechanics, Kyushu University, Kasuga, Fukuoka 816-8580, Japan*

³*National Institute for Fusion Science, Toki, Gifu 509-5292, Japan*

⁴*Interdisciplinary Graduate School of Engineering Sciences, Kyushu University, Kasuga, Fukuoka 816-8580, Japan*

(Received 16 September 2010; published 23 November 2010)

A streamer, which is a bunching of drift-wave fluctuations, and its mediator, which generates the streamer by coupling with other fluctuations, have been observed in a cylindrical magnetized plasma. Their radial structures were investigated in detail by using the biphase analysis. Their quasi-two-dimensional structures were revealed to be equivalent with a pair of fast and slow modes predicted by a nonlinear Schrödinger equation based on the Hasegawa-Mima model.

DOI: [10.1103/PhysRevLett.105.225002](https://doi.org/10.1103/PhysRevLett.105.225002)

PACS numbers: 52.35.Mw, 52.25.Xz, 52.35.Ra

The generation of mesoscale structures from gradient-driven, quasi-two-dimensional microscopic turbulence is one of the central issues in plasma physics, geofluid dynamics, physics of rapidly rotating astrophysical objects, and so on [1,2]. In the studies of magnetized plasmas, theories and simulations have predicted that drift-wave turbulence can generate the mesoscale structures, such as zonal flows (ZFs), streamers, and zonal magnetic fields (ZMs) [1–7], and the property of the drift-wave turbulence has been, in fact, revealed by recent experiments of inhomogeneous and magnetized plasmas [8–17]. These mesoscale structures, ZFs and streamers, have different behaviors, and their impacts on turbulence-driven transports show strong contrasts. For example, ZFs cause no cross-field transport owing to their symmetric structure around the axis; in contrast, streamers contribute to enhancing the transport owing to their radial elongated structure. The study of nonlinear processes, such as turbulent Reynolds stress and Maxwell stress, which induce mesoscale structures, is essential for understanding inhomogeneous and magnetized plasmas. The dynamics on the plane perpendicular to the strong mean magnetic field must be fully resolved, because the drift-wave turbulence is quasi-two dimensional. About the full two-dimensional (2D) nonlinear interaction, while a few is known of ZFs [17], there is almost no experimental knowledge for streamers.

In this article, we report our observation of streamer structure for drift-wave fluctuations in cylindrical magnetized plasmas. Bunching of drift-wave fluctuations occurs accompanied by its low-frequency mediator mode. 2D nonlinear interaction is analyzed, and the matching conditions of frequency and poloidal wave number, as well as the radially constant biphase, are confirmed. The special structure of the mediator is found in a good agreement with theoretical prediction in Ref. [4].

According to Ref. [4], a pair of fast and slow modes including a streamer structure is derived as follows. In the

Hasegawa-Mima model [18], which can give a concise description of drift-wave turbulence, the plasma density is given by $n_0 \exp \phi$, where ϕ is an electrostatic potential. When n_0 is a slowly varying function of y , the Hasegawa-Mima model equation in the coordinates (x, y) takes the form

$$\frac{\partial}{\partial t} (\Delta \phi - \phi) - \left(\frac{\partial \phi}{\partial y} \frac{\partial}{\partial x} - \frac{\partial \phi}{\partial x} \frac{\partial}{\partial y} \right) \Delta \phi - b \frac{\partial \phi}{\partial x} = 0, \quad (1)$$

where b is a constant proportional to $(dn_0/dy)/n_0$. The second nonlinear term corresponds to the turbulent Reynolds stress that can generate the mesoscale structure. When the unperturbed potential is $\phi^0 = -c_0 y$, a dc electric field exists in the y direction, the plasma drifts in the x direction, and the disturbance $\delta \phi$ is excited on the drift motion. When the fixed boundary conditions are assumed at the plasma boundaries, $\delta \phi(x, 0) = \delta \phi(x, L) = 0$ (L is the plasma length), $\delta \phi$ has the form $\delta \phi = X(x, t)Y(y)$, where $Y \propto \sin k_n y$, $k_n = n\pi/L$, and n is a natural number. It is anticipated that if $\delta \phi$ is small, wave modulations in the x direction will be described by a nonlinear Schrödinger equation. When ϕ is expressed as $\phi = \phi^0(y) + \sum_{\alpha=1} \epsilon^\alpha \phi^\alpha$, the one-soliton solution is that ϕ^1 and ϕ^2 take the forms

$$\phi^1 \propto \text{sech}[\kappa(x - \lambda t) \cos(k_x x) \sin(k_n y)], \quad (2)$$

$$\phi^2 \propto \text{sech}^2[\kappa(x - \lambda t) \sin(k_{2n} y)], \quad (3)$$

where $\lambda = d\omega/dk_x$ and κ is a function of k_x, k_n, c_0 , and b . Figure 1 shows the schematic views of contours $\phi^1 = \text{const}$ (fast mode) and $\phi^2 = \text{const}$ (slow mode). Figure 1(a) shows a train of small convective cells placing at intervals of $1/k_x$ in the x direction. The magnitudes decrease towards $|x| \rightarrow \infty$. Figure 1(b) shows a pair of vortices of large scale. When x and y are taken as the poloidal and radial directions, respectively, the fast mode becomes a streamer.

A streamer structure has been observed in the large mirror device-upgrade (LMD-U) cylindrical plasma [15].

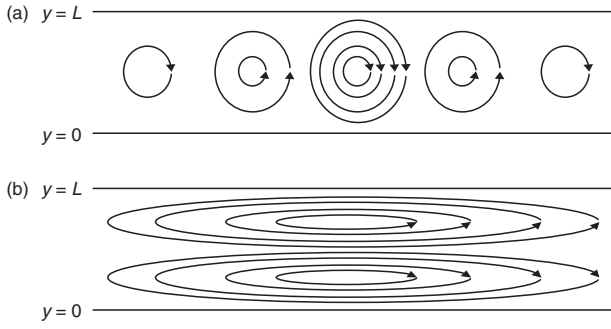


FIG. 1. Streamlines for the (a) fast and (b) slow modes derived from a nonlinear Schrödinger equation based on the Hasegawa-Mima model, with the case of $n = 1$ and $k_x = k_n$.

The LMD-U vacuum vessel has the axial length of 3.74 m. The plasma is generated by a radio-frequency wave (7 MHz, 3 kW) inside a quartz tube with an inner diameter of 95 mm. Figure 2(a) shows the spatiotemporal behavior of the ion saturation-current fluctuation measured at the radius r of 40 mm by a 64-channel poloidal probe array [19]. The discharge conditions were the filled argon pressure inside the tube of 0.2 Pa and the axial magnetic field inside the vacuum vessel of 0.09 T. With this discharge, the peak electron density of the plasma was $8 \times 10^{18} \text{ m}^{-3}$ and the electron temperature was about $3 \pm 0.5 \text{ eV}$ inside the plasma. The resistive drift-wave instability was excited by the density gradient [20] especially at around $r = 30 \text{ mm}$. A bunching of waves (streamer) is clearly seen in the spatiotemporal. It is localized in the poloidal space θ , i.e., it forms high and low-amplitude regions, and its envelope forms an $m = 1$ structure, where m is the poloidal mode number ($m \geq 0$). This $m = 1$ structure slowly rotates with the frequency f of -1.2 kHz , where negative frequency indicates the propagation in the ion diamagnetic direction. The carrier waves, which form the bunching of waves, propagate in the electron diamagnetic direction with the frequency around 8 kHz. There also exists a sinusoidal $m = 1$ wave with $f = -1.2 \text{ kHz}$, which has the same properties with the envelope of the bunching of waves. Figure 2(b) is the frequency component under 1.6 kHz extracted from Fig. 2(a). As is indicated by red lines in Fig. 2, the phase of the sinusoidal $m = 1$ wave slightly delays from that of the envelope of the bunching of waves, and these relations are always observed through the discharge. Thus, the phase locking between the $m = 1$ sinusoidal wave and bunching of waves is occurring.

Figure 3(a) is the 2D power spectrum of the spatiotemporal waveform observed in Fig. 2(a). The sampling frequency is 1 MHz, the frequency resolution of the Fourier transformation is 0.1 kHz, and the spectrum is an ensemble average of 3853 time windows. Three pronounced modes, A, B, and C, are seen in the 2D power spectrum. The mode A corresponds to the $m = 1$ sinusoidal wave observed in Fig. 2(b), and its poloidal mode number and frequency are $(m_A, f_A) = (1, -1.2 \text{ kHz})$. The modes B and C correspond

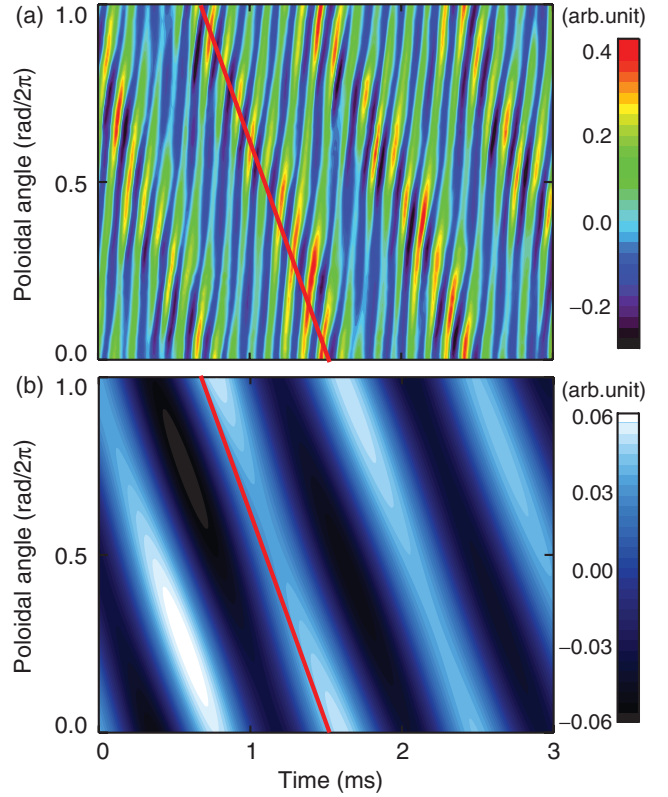


FIG. 2 (color). (a) Spatiotemporal behavior of ion saturation-current fluctuation measured with the 64-channel poloidal probe array. (b) Frequency component under 1.6 kHz extracted from (a). The phase of the bunching of waves observed in (a) is slightly faster than that of the sinusoidal wave in (b), as is indicated by red lines.

to the carrier waves which form the bunching of waves, and their mode numbers and frequencies are $(m_B, f_B) = (2, 7.8 \text{ kHz})$, and $(m_C, f_C) = (3, 6.6 \text{ kHz})$. These three modes satisfy the matching conditions $m_A + m_B = m_C$ and $f_A + f_B = f_C$. Therefore, the phase locking between them may occur and the bispectral analysis [21] can examine this. The bispectrum B of the three modes is expressed as $B = \langle Z_A Z_B Z_C^* \rangle$, where $Z_i = Z(m_i, f_i)$ is the Fourier transformed expression of mode i . The bicoherence b is a normalized value of B , and is expressed as $b^2 = |B|^2 / (\langle |Z_A Z_B|^2 \rangle \langle |Z_C|^2 \rangle)$. When the squared bicoherence b^2 becomes a finite value, the three modes exist dependently on each other, and their phases are connected by the biphas ϕ_b , which is calculated by taking the arc tangent of B . When f_B and f_C are close and larger than f_A , two modes B and C form a bunching of waves, of which the beat frequency is f_A . The biphas ϕ_b of the three modes indicates the phase difference between mode A and the envelope of the bunching of waves. For example, when $\phi_b = 0$ and π , the amplitude of the envelope is maximum when mode A is maximum and minimum, respectively. The same argument is applied in the wave number space. From calculating the ensemble average of 3853 time

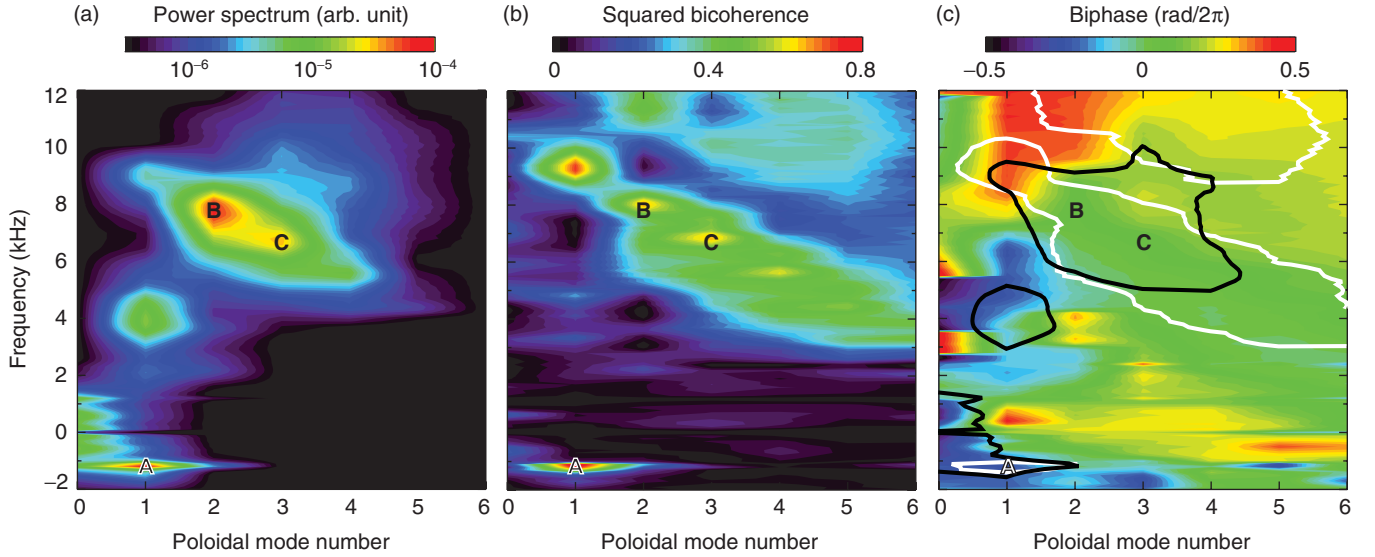


FIG. 3 (color). (a) 2D power spectrum of the ion saturation-current fluctuation observed in Fig. 2(a). Frequencies and poloidal mode numbers of three pronounced modes labeled A, B, and C are $(m, f) = (1, -1.2 \text{ kHz})$, $(2, 7.8 \text{ kHz})$, and $(3, 6.6 \text{ kHz})$. These three modes satisfy the matching condition. (b) and (c) are contours of squared bicoherence and biphase of the nonlinear coupling with the mode A, respectively.

windows, squared bicoherence b^2 was as high as 0.58, which indicated the strong nonlinear coupling between the three modes (the confidence level is $1/3853 \sim 0.0003$). The biphase ϕ_b was $0.07 \text{ rad}/2\pi$, which was slightly higher than zero. This result agrees with the observation in Fig. 2 that the phase of the mode A slightly delays from that of the envelope of the bunching of waves.

The carrier waves of the poloidally localized structure are not only the modes B and C, but also consist of many modes and even broadband fluctuations. This is because the mode A couples with many other modes and broadband fluctuations with nearly constant values of biphases ($\sim 0.1 \text{ rad}/2\pi$). Figures 3(b) and 3(c) show the squared bicoherence b^2 and biphase ϕ_b , respectively, between the three modes A, (m, f) , and $(m_A + m, f_A + f)$. The black line in Fig. 3(c) indicates where the power spectrum is 3×10^{-6} in Fig. 3(a), and the white line indicates where $b^2 = 0.3$ in Fig. 3(b). Most regions in m - f space having a large amplitude and strong coupling with A (especially for $m \geq 2$ including B and C) have the same biphase value of $\sim 0.1 \text{ rad}/2\pi$. Many accumulations of the nonlinear couplings of the carrier waves with mode A form the bunching of waves. Mode A is not a carrier wave but an important mode for forming the streamer structure and called a mediator for the formation [7].

To investigate the radial structure of the streamer, we propose a new analyzing method using the biphase between the nonlinearly coupled modes. A radially mobile probe was used in addition to the 64-channel probe array. The biphase between mode A measured with the 64-channel probe array, and modes B and C measured with the radially mobile probe, was calculated along the radial direction. In this analysis, mode A at $r = 40 \text{ mm}$

was taken as a reference, and the phase structure of the envelope of the bunching of waves (mainly formed by B and C) was determined along the radial direction through the reference. Figure 4 shows the radial profile of the biphase scanned from 10 to 60 mm. It is an ensemble-average of 59 time windows. As a result, the biphase was almost constant around $0.1 \text{ rad}/2\pi$ inside the plasma. Thus, the radially elongated structure of the streamer has been revealed in detail. Figure 4 also shows the radial phase structure of A itself. In contrast to the biphase, the phase of A suddenly jumps at $r = 30 \text{ mm}$, suggesting that mode A has a node in the radial direction.

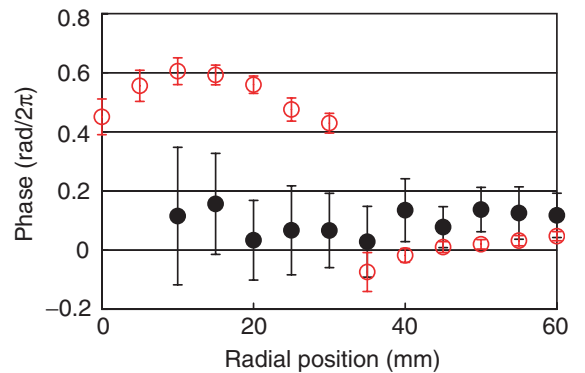


FIG. 4 (color). (Closed, black) Radial profile of the biphase between the modes A, B, and C. $Z_A = Z(m_A, f_A)$ measured with 64-channel poloidal probe array (reference signal), and $Z_B = Z(f_B)$ and $Z_C = Z(f_C)$ measured with radially mobile probe were used for the calculation. The result indicates that the poloidally localized structure has almost a radially independent structure. (Open, red) Radial profile of the phase of A, which has a node in the radial direction.

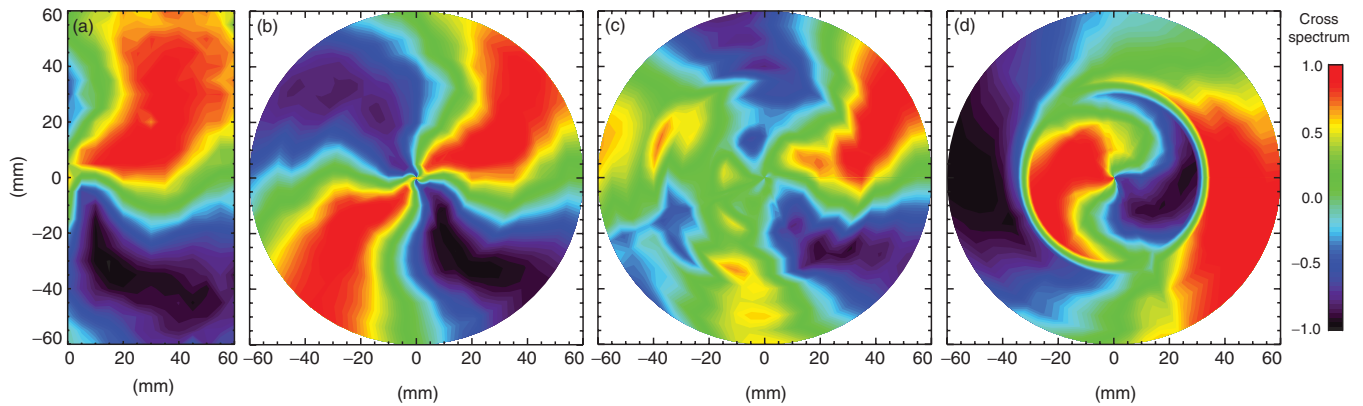


FIG. 5 (color). Contours of real parts of cross spectra between (a) 2D mobile probe and a fixed reference probe, and (b)–(d) radially mobile probe and each channel of the 64-channel probe array. Frequency ranges are (a) and (b) 7.8 kHz (including the mode B), (c) 6.6 kHz (including C), and (d) 1.2 kHz (including A). Mode A has a node in the radial direction.

Next, the spatial structure of the three modes A , B , and C themselves are investigated. Figure 5(a) shows the real part of the cross spectrum between a 2D mobile probe and a reference probe (one channel of the 64-channel probe array is used). The contour is drawn for the frequency component of 7.8 kHz, which includes the mode B . For comparison, the real part of the cross spectrum between the radial scan of the 2D mobile probe and each channel of the 64-channel probe array with the frequency component of 7.8 kHz is shown in Fig. 5(b). The results from both analyzing methods are in good agreement. Since scanning the 2D mobile probe beyond the vertical axis results in a deterioration of the plasma, the latter method is advantageous for calculating the cross spectrum for the whole plasma cross section. Figures 5(c) and 5(d) show the real parts of the cross spectra calculated with the latter method, and their frequency components are 6.6 and 1.2 kHz, which include modes C and A , respectively. As is shown in Figs. 5(a)–5(c), modes B and C , which are the carrier waves of the streamer, have radially elongated structures. In contrast, mode A , which is the mediator of the streamer, does not have a radially elongated structure. It has a node in the radial direction at $r = 30$ mm (see Fig. 4).

In short, we observed a streamer structure, and its mediator which had a node in the radial direction. Compared to Fig. 1, when x and y are taken as θ and r , respectively, the streamer structure corresponds to the fast mode, and the mediator, with the slow mode.

In summary, a streamer structure was observed in the LMD-U cylindrical plasma, and its quasi-two-dimensional structure was investigated in detail by the biphasic analysis. That is, the envelope of the turbulence formed a radially elongated global structure inside the plasma. There also existed a mediator having the same mode number and frequency with the envelope, however, it had a node in the radial direction. These features agreed well with the pair of fast and slow modes derived by a nonlinear Schrödinger equation based on the Hasegawa-Mima model in Ref. [4].

The mediator was strongly coupled with a number of streamer components with the same biphasic values.

This work was supported by Grants-in-Aid for Scientific Research of JSPS (21224014 and 21760688), the collaboration programs of NIFS (NIFS10KOAP023) and RIAM, Kyushu University, and the Asada Eiichi Research Foundation.

*takuma@k.u-tokyo.ac.jp

- [1] P. H. Diamond *et al.*, *Plasma Phys. Controlled Fusion* **47**, R35 (2005).
- [2] *The Solar Tachocline*, edited by D. Hughes, R. Rosner, and N. Weiss (Cambridge University Press, Cambridge, U.K., 2007).
- [3] V. I. Petviashvili, *Sov. J. Plasma Phys.* **3**, 150 (1977).
- [4] K. Nozaki, T. Taniuti, and K. Watanabe, *J. Phys. Soc. Jpn.* **46**, 991 (1979).
- [5] J. F. Drake, A. Zeiler, and D. Biskamp, *Phys. Rev. Lett.* **75**, 4222 (1995).
- [6] S. Champeaux and P. H. Diamond, *Phys. Lett. A* **288**, 214 (2001).
- [7] N. Kasuya *et al.*, *Phys. Plasmas* **15**, 052302 (2008).
- [8] P. A. Politzer, *Phys. Rev. Lett.* **84**, 1192 (2000).
- [9] A. Fujisawa *et al.*, *Phys. Rev. Lett.* **93**, 165002 (2004).
- [10] Y. Nagashima *et al.*, *Phys. Rev. Lett.* **95**, 095002 (2005).
- [11] G. R. Tynan *et al.*, *Plasma Phys. Controlled Fusion* **48**, S51 (2006).
- [12] C. Hidalgo *et al.*, *Plasma Phys. Controlled Fusion* **48**, S169 (2006).
- [13] C. Holland *et al.*, *Phys. Rev. Lett.* **96**, 195002 (2006).
- [14] Y. Hamada *et al.*, *Phys. Rev. Lett.* **96**, 115003 (2006).
- [15] T. Yamada *et al.*, *Nature Phys.* **4**, 721 (2008).
- [16] A. Fujisawa, *Nucl. Fusion* **49**, 013001 (2009).
- [17] Y. Nagashima *et al.*, *Phys. Plasmas* **16**, 020706 (2009).
- [18] A. Hasegawa and K. Mima, *Phys. Rev. Lett.* **39**, 205 (1977).
- [19] T. Yamada *et al.*, *Rev. Sci. Instrum.* **78**, 123501 (2007).
- [20] T. Yamada *et al.*, *Phys. Plasmas* **17**, 052313 (2010).
- [21] Y. C. Kim and E. J. Powers, *Phys. Fluids* **21**, 1452 (1978).